

Pd–Fe Nanoparticles as Electrocatalysts for Oxygen Reduction

Min-Hua Shao, Kotaro Sasaki, and Radoslav R. Adzic*

Chemistry Department, Brookhaven National Laboratory, Upton, New York 11973

Received January 9, 2006; E-mail: adzic@bnl.gov

Recent efforts in electrocatalysis have focused on decreasing the Pt content in fuel cell electrocatalysts or replacing it with less expensive materials.¹ We report on a new electrocatalyst that does not contain Pt; it consists of Pd–Fe alloy nanoparticles and has a very high activity for the oxygen reduction reaction (ORR). Pd is considerably less expensive than Pt, but less active for the ORR. Our previous work on palladium alloy electrocatalysts demonstrated that Pd/C nanoparticles modified with Co become very active for the ORR.² Others reported similar activity for sputtered Pd–Co films³ and for Pd–Co–Au alloy nanoparticles.^{3,4} Enhancing further the catalytic activity and stability of Pd for the ORR is of considerable interest, and replacing Pt with an inexpensive Pd-noble-metal alloy could facilitate faster and broader application of fuel cells.

Pd–Fe/C electrocatalysts with a molar ratio of Pd:Fe from 1:1 to 4:1 were prepared by thermal treatment. The mixture of 19 wt % Pd/C nanoparticles of average diameter, 4.8 nm (E-TEK), and FeCl₃ solution was dried at 80 °C and heated in H₂ at 400–850 °C for 2.5 h. For comparison, Pd–Fe/C nanoparticles also were prepared by thermal decomposition of the mixture of PdCl₂ and FeCl₃ salts on carbon particles (Vulcan XC-72). The total metal loading (Pd plus Fe) varied from 20.9 (Pd₄Fe/C) to 26.4 wt % (PdFe/C). An electrocatalyst thin film covered with a thin layer of Nafion was cast on a glassy carbon disk electrode (5 mm diameter) for the ORR measurements.

The results, obtained as a function of temperature, showed that the Pd–Fe/C alloys treated at 500 °C have the highest ORR activity; hereafter, only these are discussed. Their structures were determined from X-ray diffraction data (Figure S1). All the Pd–Fe/C alloys showed a typical fcc pattern with diffraction angles shifting to higher positions compared to those of Pd/C. These angular shifts reflect lattice contraction due to the replacement of part of Pd with Fe. Table 1 lists the particle sizes and the corresponding Pd–Pd bond distances calculated from the (220) diffraction line using the Scherrer formula and Bragg equation, respectively. The lattice constant decreases in the order Pd > PdFe ≈ Pd₂Fe > Pd₄Fe > Pd₃Fe. From the phase diagram,⁵ we deduced that the ordered Pd₃–Fe (L1₂-type) phase with an fcc structure is favored in the composition range of 65–85 atom % Pd at 500 °C, while an ordered tetragonal PdFe (L1₀-type) appears in the range of 50–60 atom % Pd. PdFe/C was the only sample showing a weak PdFe superlattice reflection. This may indicate that the phase ordering in PdFe nanoparticles does not readily occur, which is in agreement with earlier observations.⁶ However, we cannot exclude the existence of a superlattice in other Pd–Fe/C particles because of the weak superlattice signals.

Figure 1 displays the ORR polarization curves for Pd₃Fe/C, Pd/C, and Pt/C in O₂-saturated 0.1 M HClO₄ solution obtained using a rotating disk electrode at 1600 rpm. The curve of Pd₃Fe/C shows a 70 mV shift to more positive potentials compared with Pd/C. Furthermore, the activity of Pd₃Fe/C is higher than that of the state-of-the-art commercial Pt/C electrocatalyst. The respective half-wave

Table 1. Structural and Electrochemical Characteristics of the Pd/C and Pd–Fe/C Electrocatalysts

sample	particle size (nm)	Pd–Pd bond distance (nm)	electrochemical area ^a (cm ² mg ⁻¹ _{Pd})	<i>j</i> _k at 0.85 V ^b (mA cm ⁻²)
Pd/C	10.2	0.2753	446	0.131
Pd ₄ Fe/C	9.6	0.2735	501	0.500
Pd ₃ Fe/C	9.7	0.2730	726	0.791
Pd ₂ Fe/C	7.6	0.2742	874	0.346
PdFe/C	7.7	0.2743	721	0.420
Pd ₃ Fe/C ^c	7.3	0.2747	546	0.268

^a Using the charge for H_{upd} of 210 μC cm⁻². ^b Normalized to the electrochemical area. ^c Prepared by heat decomposition of PdCl₂ and FeCl₃ salt mixtures.

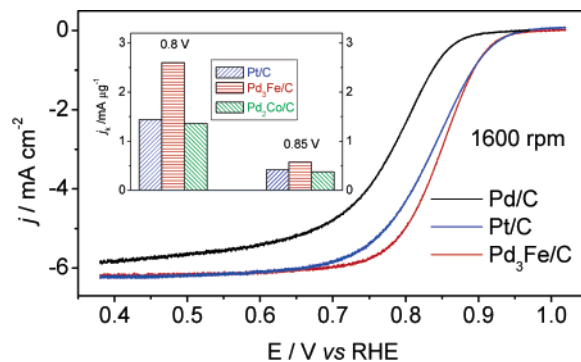


Figure 1. Polarization curves for the ORR on Pd/C (E-TEK), Pt/C (E-TEK), and Pd₃Fe/C nanoparticles in 0.1 M HClO₄. Sweep rate = 10 mV s⁻¹; room temperature. The Pd or Pt loading is 10 μg cm⁻². Inset: Comparison of mass activity for Pt/C (E-TEK), Pd₃Fe/C, and Pd₂Co/C at 0.8 and 0.85 V. The data for Pd₂Co/C are taken from ref 2.

potentials are 848 and 835 mV. The ORR onset potentials are similar for these two surfaces. The inset in Figure 1 shows their mass activity that is a better indicator of an electrocatalysts' quality. The mass activity of Pd₃Fe is 1.4 and 1.9 times higher than that of a commercial Pt/C electrocatalyst at 0.85 and 0.8 V, respectively. The enhancement would probably be considerably higher were the electrocatalysts of the same particle size. This comparison favors Pt/C having a larger surface area due to its higher dispersion (2.8 nm for Pt/C vs 9.7 nm for Pd₃Fe/C). Pd₃Fe/C is also twice as active as Pd₂Co/C at 0.8 V, which has the highest activity among the Pd–Co/C catalysts.²

Figure 2 plots the voltammetry curves of Pd₃Fe/C and Pd/C, both of similar particle size and treated at 500 °C. Interestingly, the current densities in the hydrogen adsorption/desorption and oxide formation/reduction regions of Pd₃Fe/C are larger than those of Pd/C. The specific electrochemical areas of nanoparticles, calculated from the H_{upd},⁷ assuming Fe has no effect on hydrogen adsorption/desorption behavior, are listed in Table 1.

Larger electrochemical areas are observed for all the Pd–Fe/C alloys than that of Pd/C, indicating that rough surfaces are formed during alloying. The invariability of voltammetry during several cycles means that leaching of Fe atoms from the surface layer does

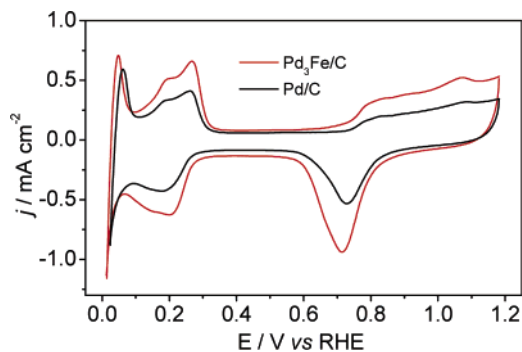


Figure 2. Cyclic voltammograms of Pd₃Fe/C and Pd/C in N₂-saturated 0.05 M H₂SO₄ solution. Sweep rate = 50 mV s⁻¹; Pd loading = 10 μg cm⁻².

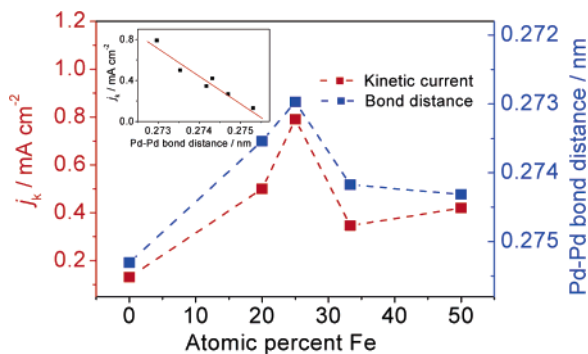


Figure 3. Kinetic current density (electrochemical area) and Pd–Pd bond distance calculated from XRD data against the concentration of Fe in Pd–Fe/C electrocatalysts treated at 500 °C.

not cause the roughness (larger surface area). It may play a role in enhancing the kinetics of the ORR observed for Pd–Fe/C. However, it is not its only cause as the kinetic current density, normalized to the electrochemical area (surface-specific activity), is still much higher than that of Pd/C.

We analyzed the relationship between surface-specific activity (j_k) and Pd–Pd bond distance to gain more information on the enhanced activity of the alloys and the possible role of their structure (Figure 3). A good parallelism is observed between j_k and the Pd–Pd interatomic distance expressed as a function of the alloy's composition; this distance plot, given as an inset, revealed a clear correlation between the two variables. The highest ORR activity is obtained for a 0.273 nm Pd–Pd bond distance. For some Pt–M alloys, the peak in activity was observed for an optimal Pt–Pt bond distance.⁸ The relationship between j_k and Pd–Pd bond distance is corroborated by the low activity of Pd₃Fe/C prepared by heating a PdCl₂ and FeCl₃ mixture wherein the Pd–Pd distance is 0.2747 nm, larger than 0.273 nm. Establishing the origin of the effect of different synthesis methods on the activity of the Pd₃Fe electrocatalyst is beyond the scope of this work. It requires further study.

Different bond lengths generate strains, thereby modifying the electronic structure of the metal through changes in orbital overlap that, in turn, alter the d-band center, which determines surfaces' reactivity.⁹ The density functional theory (DFT) calculations indicate that compression of a Pd lattice in PdFe alloys will downshift the

d-band center by -0.88 eV.¹⁰ Pd is a relatively reactive metal. It oxidizes at more negative potentials than Pt; thus, its position is on the ascending branch of the volcano plot for the ORR below Pt.¹¹ Therefore, decreasing the activity of Pd could lower the blocking effect of O₂, O/OH, O₂⁻, and H₂O₂ by weakening their bonding to Pd. This process enhances ORR kinetics. Thermodynamically, Wang and Balbuena¹² predicted an ORR would be enhanced by coupling a metal M (M = Co, Ni, Cr, V, and others) with low occupancy of d-orbitals with another metal M' (such as M' = Pd, Au, and Ag) with fully occupied d-orbitals. The enhancement arises from decreasing the Gibbs free energy of the electron transfer steps with alloying.

One of the major problems in direct methanol fuel cells (DMFCs) is the crossover of methanol to the cathode and the need for methanol tolerance in the cathode catalysts to ensure a good performance. Figure S2 depicts the much lower activity of Pd₃Fe/C for methanol oxidation than that of Pt/C. Thus, in an ORR test, Pd₃Fe/C is proved very stable; the presence of 0.1 M methanol in an acidic solution caused a negative shift of only 10 mV in its half-wave potential (Figure S3).

In conclusion, we demonstrated the synthesis of a new class of electrocatalysts consisting of Pd–Fe alloys. We showed that an active ORR electrocatalyst can be devised without Pt. Its activity can surpass that of the state-of-the-art carbon-supported Pt electrocatalysts. With the lower price of Pd compared to Pt, and the possibility of using two metals instead one as the electrocatalyst, the cost of fuel cells could be lowered considerably. Further work on these systems will address the question of their long-term stability.

Acknowledgment. This work is supported by U.S. Department of Energy, Divisions of Chemical and Material Sciences, under the Contract No. DE-AC02-98CH10886. The authors appreciate valuable discussions with J.X. Wang and H.S. Isaacs. M.-H.S. acknowledges partial support from Department of Materials Science and Engineering, State University of New York at Stony Brook.

Supporting Information Available: Experimental procedures and supporting figures. This material is available free of charge via the Internet at <http://pubs.acs.org>.

References

- (1) Markovic, N. M.; Schmidt, T. J.; Stamenkovic, V.; Ross, P. N. *Fuel Cells* **2001**, *1*, 105.
- (2) (a) Adzic, R. R. In *DOE Hydrogen and Fuel Cell Review Meeting*; Philadelphia, PA, 2004. (b) Adzic, R. R.; Huang, T. U.S. Patent pending.
- (3) Savadogo, O.; Lee, K.; Oishi, K.; Mitsushimas, S.; Kamiya, N.; Ota, K.-I. *Electrochem. Commun.* **2004**, *6*, 105.
- (4) Fernandez, J. L.; Walsh, D. A.; Bard, A. J. *J. Am. Chem. Soc.* **2005**, *127*, 357.
- (5) Hansen, M. *Constitution of Binary Alloys*; McGraw-Hill: New York, 1958; pp 696–698.
- (6) Chen, M.; Nikles D. E. *J. Appl. Phys.* **2002**, *91*, 10.
- (7) Correia, A. N.; Mascara, L. H.; Machado, S. A. S.; Avaca, L. A. *Electrochim. Acta* **1997**, *42*, 493.
- (8) Mukerjee, S.; Srinivasan, S.; Soriaga, M. P.; McBreen, J. J. *Electrochem. Soc.* **1995**, *142*, 1409.
- (9) Hammer, B.; Norskov, J. K. *Adv. Catal.* **2000**, *45*, 71.
- (10) Greeley, J.; Norskov, J. K. *Surf. Sci.* **2005**, *592*, 104.
- (11) Norskov, J. K.; Rossmeisel, J.; Logadottir, A.; Lindqvist, L.; Kitchin, J. R.; Bliigaard, T.; Jonsson, H. *J. Phys. Chem. B* **2004**, *108*, 17886.
- (12) Wang, Y. X.; Balbuena, P. B. *J. Phys. Chem. B* **2005**, *109*, 1890.

JA060167D